IV. RADIO ASTRONOMY*

Academic and Research Staff

Prof. A. H. Barrett
Prof. B. F. Burke
Prof. M. Loewenthal
Prof. L. B. Lenoir
Prof. D. H. Staelin
Dr. S. H. Zisk
Patricia P. Crowther
E. R. Jensen

Graduate Students

R. J. Allen
N. E. Gaut
J. M. Moran, Jr.
G. D. Papadopoulos
E. C. Reifenstein III
A. E. E. Rogers
K. D. Thompson
T. L. Wilson

A. ABSOLUTE FLUX MEASUREMENTS OF CASSIOPEIA A AND TAURUS A AT 3.64 AND 1.94 CM

1. Introduction

During December 1965 and January 1966, a series of observations of the two strong radio sources Cassiopeia A and Taurus A was conducted at the Haystack Research Facility of Lincoln Laboratory, M.I.T. The antenna, a cornucopia horn reflector of approximately 6 m^2 aperture, has been measured extensively on a ground reflection antenna pattern range. Drift-scan observations were made at transit for both sources at two frequencies, 8.25 GHz and 15.50 GHz. The radiometers were examined for nonlinearity, and the gas-tube noise calibration sources were referred to standard terminations at liquid-nitrogen temperature. Data were collected on punched paper tape, and drift scans were individually processed on a digital computer. After baseline subtraction and scaling, each scan was approximated by a one-dimensional Gaussian curve through an iteration procedure, with the use of a set of equations developed from the minimum least-squares error criterion. The data were corrected for atmospheric attenuation, waveguide losses, integration time constant, source size, and, in the case of Taurus A, polarization, then converted to absolute flux by using the measured efficiency of the antenna.

Although mention of this work has been made in a previous progress report,[1] the present report constitutes a full description of the measurement techniques and the method of data reduction.

*This work was supported principally by the National Aeronautics and Space Administration (Grant NsG-419 and Contract NSR-22-009-120); and in part by Lincoln Laboratory Purchase Order No. 748.

2. System Parameters

a. Aperture Efficiency of the Horn Antenna

Measurements of the gain of the cornucopia antenna from 2.7 to 16.0 GHz were performed by A. Sotiropoulos. The substitution method was used on a simulated free-space range. The data have been analyzed by A. Sotiropoulos and J. Ruze, of Lincoln Laboratory, and their results have been published in a technical report.[2] The conclusions pertinent to the present observations are presented in Table IV-1, where η = aperture efficiency, defined as the ratio of the effective area to the actual area of the aperture $A\hat{g}$. The quantity $\rho = 2k/\eta A\hat{g}$ is the number that converts antenna temperature from an unpolarized point source to flux in units of 10^{-26} Wm^{-2} Hz^{-1} according to $S\hat{\nu} = \rho T_A$. Because of uncertainties in the measurement of η, the quantity ρ has an rms error of 4 per cent at both frequencies.

Table IV-1. Results.

Frequency (GHz)	η	ρ
8.25	0.719 ± .028	633 ± 25
15.50	0.578 ± .023	787 ± 31

b. Rotary Joint and Waveguide Losses

The cornucopia antenna is mounted in such a way as to allow rotation about its longitudinal axis. Figure IV-1 shows the arrangement. The rotational axis is aligned East-West, so that the antenna beam is movable in elevation along the meridian plane. The radiometric instrument box is shown attached to the antenna. The antenna is connected to the radiometer through a rotary joint, a 6-inch piece of flexible waveguide, and a 6-inch piece of solid waveguide. Figure IV-2 shows the arrangement.

The calibrations of the radiometer were referred to the indicated flange (Fig. IV-2). To account for the loss plus VSWR combination of the rotary joint and connecting waveguide, the following measurements were taken at both frequencies: The antenna was replaced with a gas-tube noise source and connected to the rotary joint through a precision attenuator. The radiometer was left attached to the connecting waveguide. The precision attenuator was then varied and the temperatures measured by the radiometer were recorded at T_a. The second step was to remove

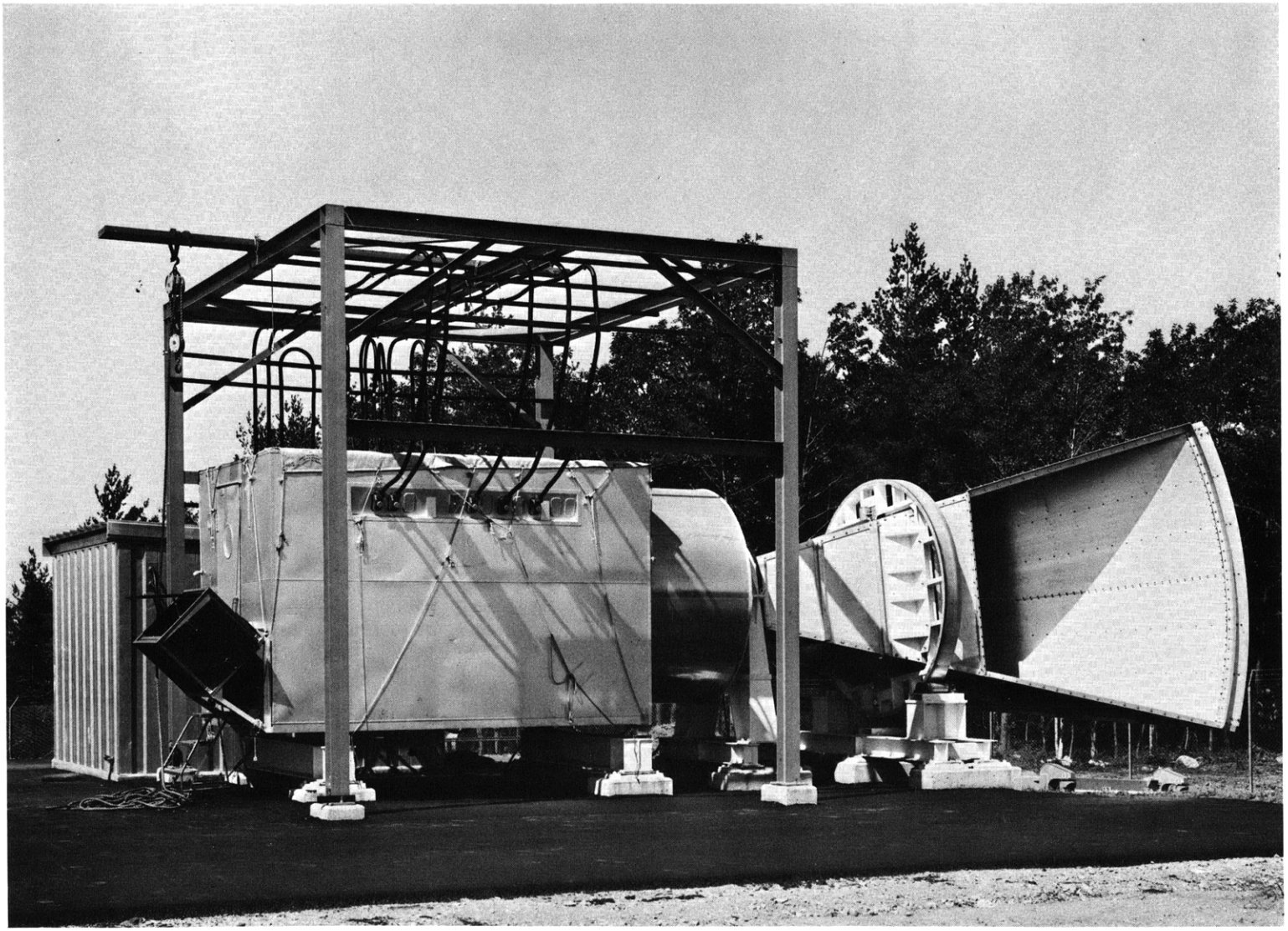

Fig. IV-1. Cornucopia horn-reflector antenna. The radiometers are housed in the boxlike room on the left, which is approximately 8 ft high.

the rotary joint and waveguide, and connect the precision attenuator directly to the calibration flange of the radiometer. The attenuator was then varied through the same

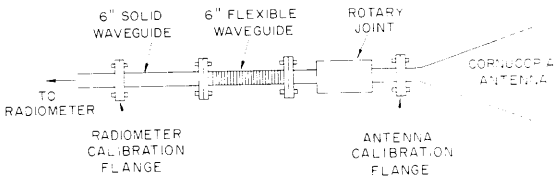

Fig. IV-2. Sketch of the plumbing between the antenna and radiometer.

values as before, and the radiometer output recorded as T_o. The slope of the graph of T_o vs T_a then yields the quantity and the correction factor desired. The results are given in Table IV-2.

Table IV-2. Results.

Frequency (GHz)	α
8.25	1.049 ± 0.005
15.50	1.062 ± 0.007

The uncertainty in α arises from the slight changes as the rotary joint is rotated. The error quoted is the maximum deviation that was found.

c. Radiometer System

The radiometric system was designed by S. Weinreb, and built at Lincoln Laboratory. A description has been given elsewhere.[3] Briefly, the radiometers at both frequencies are simple Dicke-switched t. r. f. receivers, employing a cascade of wideband tunnel-diode amplifiers followed by a travelling-wave tube amplifier. The amplifiers have 1000-MHz bandwidth. The signal at the output of the final RF amplifier is split into two 500-MHz bands (as an aid in identifying interference) and delivered to the square-law detectors. Figure IV-3 shows the control panel for one of the radiometers with a block diagram of the RF components. After square-law detection, the signals are synchronously demodulated and applied to linear integrators.

The equivalent noise temperature of the radiometer was calculated by measuring the over-all sensitivity as a function of integration time, with the radiometer balanced on a room-temperature load. The relevant equation is

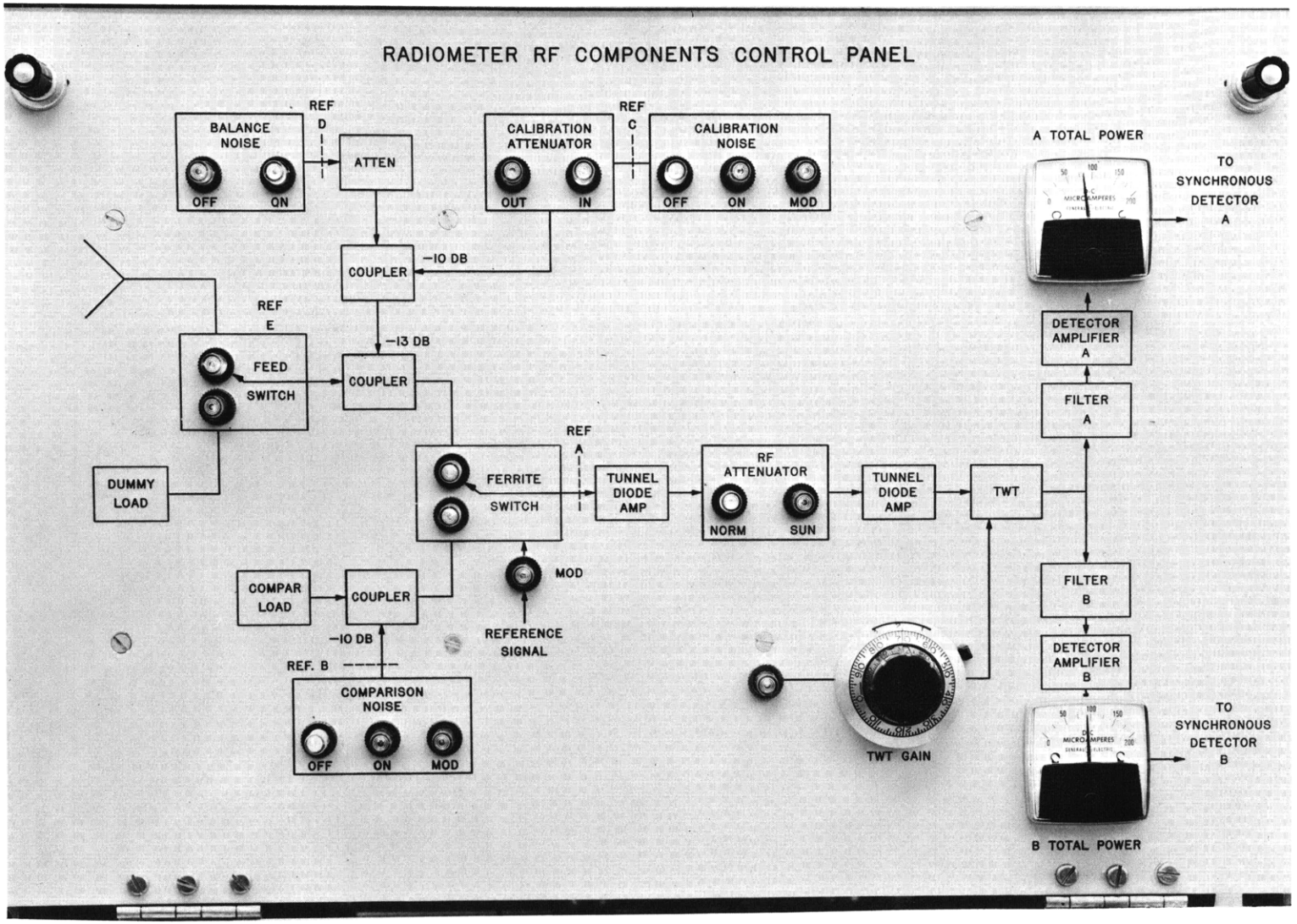

Fig. IV-3. Control panel for the radiometer, showing a block diagram of the RF components.

$$(\Delta T)\text{rms} = \frac{2(T_R + T_a)}{\sqrt{B\tau}},$$

where

(ΔT)rms = Root-Mean-Square noise fluctuation, measured in °K

T_R = equivalent receiver noise temperature, °K

T_a = temperature of the load attached to radiometer input, °K

B = system bandwidth in Hz

τ = integration time in seconds.

A plot of log (ΔT)rms vs τ should yield a straight line of slope $-1/2$, and the intercept at $\tau = 1$ sec allows a determination of T_R. Figure IV-4 shows the graphs for a 500-MHz band centered at each of two frequencies, 8.25 GHz and 15.75 GHz.

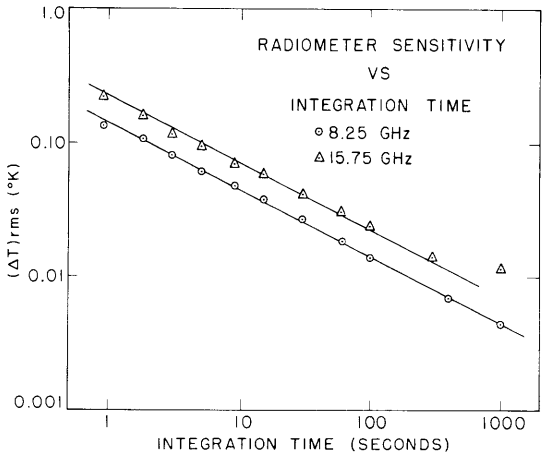

Fig. IV-4. Dependence of sensitivity on integration time. A straight line of slope $-1/2$ has been run through the points.

The 500-MHz channel centered at 7.75 GHz is usually severely hampered by interference; the two 500-MHz channels at 15.25 and 15.75 GHz are averaged together after processing. Table IV-3 lists the relevant parameters for the radiometers. The great stability of these radiometers is exhibited in Fig. IV-5, which shows a histogram of

Table IV-3. Radiometer parameters.

Quantity	Center Frequency (GHz) 8.25	15.50	Units
Bandwidth B	500	1000	MHz
Noise Temperature T_R	1300	2150	°K
Sensitivity for τ = 1 sec	0.10	0.16	°K

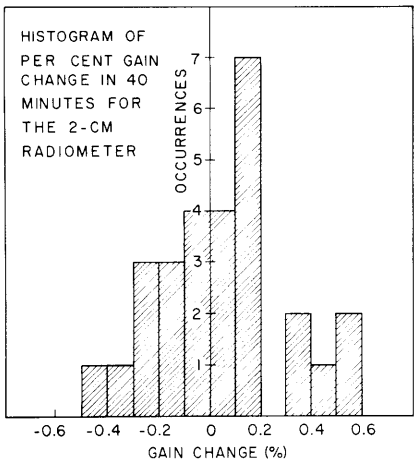

Fig. IV-5. Histogram of the per cent gain change in a 40-minute time interval for the 2-cm radiometer.

gain change of the 15.50-GHz system over a 40-minute time interval.

The over-all linearity of the system was investigated in the following manner: A gas-discharge noise source was connected to the radiometer through a precision variable attenuator, and the synchronous detector output voltage recorded at various settings of this attenuator. Signals from zero to approximately 30°K were used, since this figure is approximately the size of the calibration signal in the radiometer. Because of the high noise temperature of the radiometer, departures from linearity with such a relatively small input signal should be negligible, and the measurements bear this out. Let us assume that a reasonable representation of the relationship between the synchronous detector output voltage V_o and the input signal T_i in °K, after subtracting the baseline, is

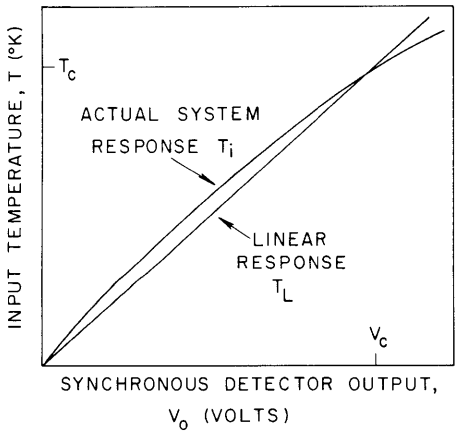

Fig. IV-6. Sketch of a possible departure from linearity in the radiometric system.

$$T_i = aV_o = bV_o^2. \qquad (1)$$

We desire to evaluate the correction factor to be applied to the data under the assumption that the detector output voltage V_o and the input signal T_i are linearly related by

$$T_{iL} = cV_o. \qquad (2)$$

The effects of nonlinearity are represented by the b coefficient in Eq. 1. The coefficient c of Eq. 2 is chosen so that both equations yield the calibration signal, T_{CAL}, when the detector output voltage is V_c. Figure IV-6 clarifies the procedure. Equating Eqs. 1 and 2 with $V_o = V_c$ gives

$$a = c - bV_c.$$

When this is used in Eq. 1 it gives

$$T_i = \left[1 - \frac{b}{c}(V_c - V_o)\right] T_{iL} \equiv \beta T_{iL}.$$

For the observations reported here, V_c = 8.5 volts, V_o = 0.2 volt (typical). Values of a, b, c, and β, determined from measurements, are given in Table IV-4. As expected, the correction for nonlinearity β is less than 1 per cent and was neglected in the subsequent analysis.

Table IV-4. Values determined from measurements.

Frequency	a	b	c	β
GHz	°K/volt	°K/(volt)^2	°K/volt	
8.25	3.37	2.46×10^{-3}	3.39	0.994
15.5	3.04	3.36×10^{-4}	3.04	0.999

The temperature of the calibration noise tube in each radiometer was referred to the difference between a room-temperature load and a termination at the temperature of liquid nitrogen.[4] The accuracy of the measurement hinges on the uncertainty of the value of the temperature at the input flange of the cold load. After correction for VSWR, this amounts to 0.5°K at 8.25 GHz, and less than 1°K at 15.50 GHz. Since the hot-cold load temperature difference ≈215°K, this error is less than 0.5 per cent at both frequencies. A measurement of the calibration noise temperature consisted of allowing the gas tube to warm up for 10 seconds, and then averaging the output for precisely 2 minutes. This procedure was necessary, since the noise temperature of the tube was found to decrease slightly with time in a very reproducible fashion, an effect which has been noticed previously in gas discharges. Table IV-5 shows the results of measurements separated by a 3-month time interval.

Table IV-5. Results of measurements.

	Frequency (GHz)			
Date	7.75	8.25	15.25	15.75
October 7, 1965	29.37°K	28.87°K	25.74°K	26.08°K
Jan. 18, 1966	29.14°K	28.72°K	25.68°K	25.85°K

It is notable that the calibration signals on January 18, 1966, differed in all cases

by less than 1 per cent from the values on October 7, 1965. With these values of calibration temperatures taken, the 15.5-GHz radiometer was used to measure the temperature of a termination immersed in a slush mixture of melting ice, and the results compared with temperatures on a mercury thermometer. Including the mismatch at the load, the radiometric temperature was 20.96 ± 0.05°C (rms error), whereas the mercury thermometer read 21.0°C. The agreement substantiates the "less than 1%" error estimate of the calibration-noise temperature.

3. Observations

An attempt to begin measurements was thwarted, in 1964, by a bewildering lack of reproducibility in the data. The trouble was traced to a faulty antenna elevation indicator. The solution consisted in first fastening a scribed reference block on the stationary part of the antenna mount, close to the large support ring, (see Fig. IV-1). Next, a reference marker was attached to the movable support ring at the nominal elevation of transit for each radio source, thereby making a "setting circle." Because of the large diameter of the ring, 1/32 inch on the reference marker is equivalent to 2.20 minutes of arc. The reproducibility of aligning a given reference mark with the scribed block is estimated to be better than 20 seconds of arc – quite adequate for the job.

An observation consists of the following sequence of events: The horn antenna is elevated to the desired setting on the reference marker. The paper tape punch is started, and begins recording the output of the linear integrators every 10 seconds. Approximately 20 minutes before the source is due to transit, the calibration noise tube is turned on for 2 minutes. The source then drifts through the antenna beam, and 20 minutes later the noise tube is turned on again. Figure IV-7 shows the analog record of a typical observation.

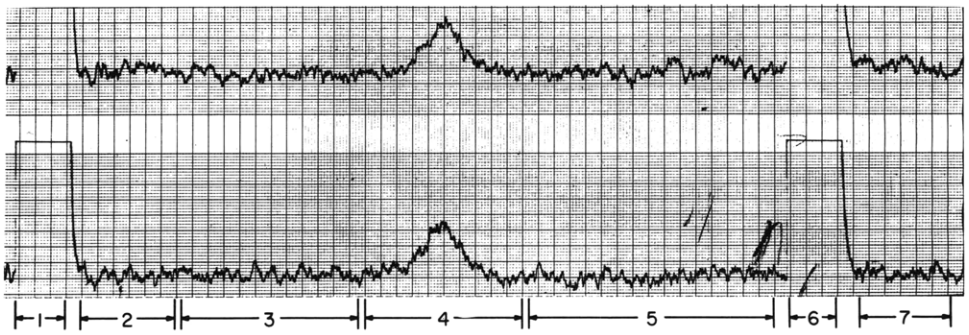

Fig. IV-7. Drift scan of Taurus A at 2 cm with the cornucopia horn atenna on January 16, 1966. The recording time constant is 10 seconds, and the time lapse from region 1 to region 6 is approximately 40 minutes.

The calibration is off-scale on the analog records, but is recorded correctly on the paper tape punch. The signal shown is approximately 0.4°K, and the recorder RC time constant is 10 seconds. Transit drift scans were taken of each source at each frequency at various elevation offsets as measured on the reference marker.

4. Data Reduction

A computer program was written to process the data automatically. The computer first reads the tape, recording and numbering the incoming data points sequentially, and produces a plot of signal versus point number on the high-speed printer. The observer then examines the analog record (see Fig. IV-7) to decide which parts of the observation

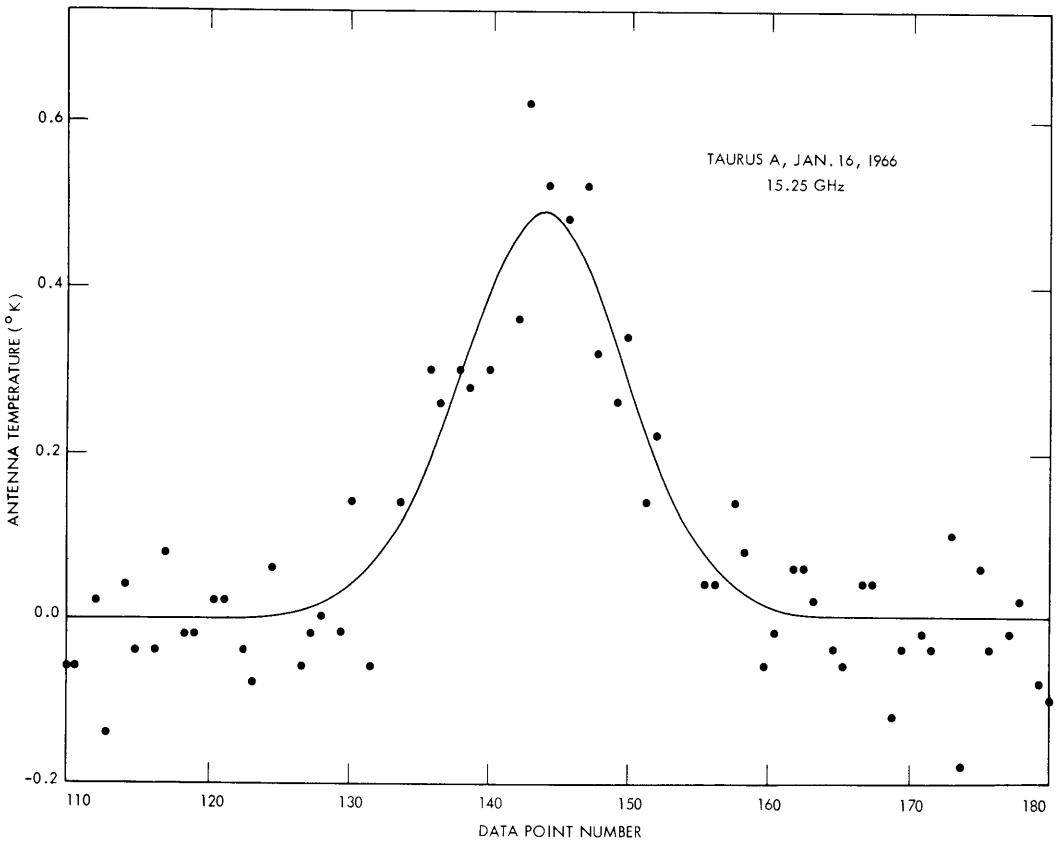

Fig. IV-8. Region 4 from Fig. IV-7, showing the data points and the Gaussian curve fitted through them by the computer program.

are to be considered as calibration, baseline, and transit data. Upon correlating the analog record with the printer plot, the observer then informs the computer of the point number for the beginning and end of each type of data. Figure IV-7 is marked off in the relevant ranges as follows:

1. First calibration signal.
2. Baseline for first calibration signal.
3. Baseline for observation before transit.
4. Transit of radio source.
5. Baseline for observation after transit.
6. Second calibration signal.
7. Baseline for second calibration signal.

The program then averages the signals for the first calibration and subtracts the average signal on the first calibration baseline. The same operation is done on the second calibration. Using the value of this calibration in degrees Kelvin, the computer proceeds to correct the data between the calibrations for any linear gain changes (a procedure later found to be unnecessary) and scales the numbers to temperature. Then, the two blocks of data labelled "baseline" before and after transit are fitted by least squares to a straight line and this baseline subtracted from the transit data. The uncorrected transit observation is then fitted by a least-squares iteration procedure to a Gaussian curve, and the results are printed out. Figure 8 shows the curve calculated from the corrected data of Fig. IV-7.

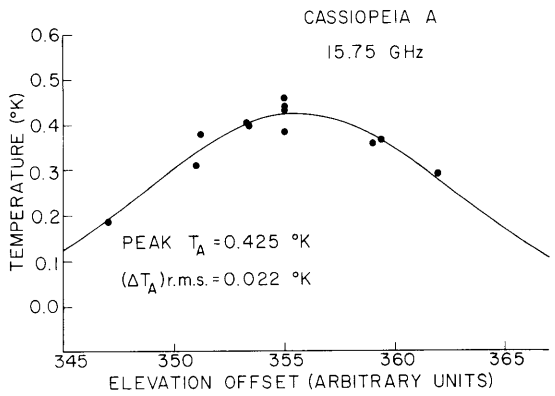

Fig. IV-9.
Peak temperatures of all drift scans on Cassiopeia A at 15.75 GHz. Solid curve is the least-squares Gaussian curve through the data points.

Each run is corrected individually for atmospheric attenuation. Ground-level relative humidity is monitored at the radio telescope site and the total atmospheric attenuation is determined from theoretical expressions. Typical zenith attenuations, during wintertime conditions, amounted to 1.8 per cent at 8.25 GHz and 2.5 per cent at 15.5 GHz.

The peak temperatures for all runs at all different elevation offsets are then fitted to another Gaussian by the same program to yield finally the peak temperature for the source. Figure IV-9 shows the data and the computed curve for one of the sources.

5. Results

The results of all of these measurements are best presented in tabular form.

Table IV-6. Results of measurements for Cass A.

Cassiopeia A	Frequency (GHz)			
Quantity	8.25	15.25	15.75	Comments
$\Delta\alpha$ (arc minutes)	45.9	30.0	30.0	Right Ascension response width
$\Delta\delta$ (arc minutes)	59.4	28.2	35.3	Declination response width
Peak temperature (°K)	0.925	0.479	0.425	Parallactic angle of feed = 90°
(ΔT) rms	0.004	0.025	0.022	
Rotary joint loss	1.049	1.062	1.062	Correction factors
10-sec linear integrator	1.000	1.000	1.000	See Note
Source size	1.002	1.008	1.008	
Total correction factor	1.051	1.070	1.070	
Corrected temperature	0.972	0.512	0.455	Degrees Kelvin
Flux $S\nu$	616	399	362	Units 10^{-26} Wm^{-2} Hz^{-1}
Total rms error (%)	4.5	6.5	6.5	See Table IV-8
Epoch	1965.9	1966.0	1966.0	

Note: The source size correction used for Cassiopeia A is the mean of the correction factors for a disc 4:0 diameter and for a thin ring 4:0 diameter. The beamwidths used in this calculation were the response widths in Right Ascension and Declination listed in Tables IV-6 and IV-7.

Table IV-7. Results of measurements for Tau A.

Taurus A	Frequency (GHz)			
Quantity	8.25	15.25	15.75	Comments
$\Delta\alpha$ (arc minutes)	47.1	31.3	31.1	Right Ascension response width
$\Delta\delta$ (arc minutes)	58.0	34.0	35.8	Declination response width
Peak temperature (°K)	0.822	0.548	0.507	Parallactic angle of feed = 90°
(ΔT) rms	0.005	0.029	0.022	
Rotary joint loss	1.049	1.062	1.062	
10-sec linear integrator	1.000	1.000	1.000	
Source size	1.0047	1.0120	1.0120	4:2 × 2:9 Gaussian
Polarization	1.033	1.033	1.033	See Note
Total correction factor	1.0887	1.110	1.110	
Corrected temperature	0.895	0.608	0.563	
Flux $S\nu$	567	474	448	
Total rms error (%)	4.5	6.5	6.5	See Table IV-8
Epoch	1966.0	1966.0	1966.0	

Note: The polarization averaged over the source Taurus A at 8.25 GHz has been measured with the Haystack antenna to be 8.0% at parallactic angle 147°. The recent data of Boland et al.[5] at 2.07 cm indicate that the same correction factor may be applied to the present data at 15.5 GHz.

Table IV-6 shows the results for Cassiopeia A, and Table IV-7 the results for Taurus A. The rms errors involved in the final result are listed in Table IV-8 in percentages.

Table IV-8. RMS errors.

Description of Source of Error	Frequency (GHz) 8.25	15.50
Measurement of peak temperature	0.7%	5.0%
Rotary joint losses (rotation)	0.5	0.7
Source model	0.2	0.3
Antenna efficiency	4.0	4.0
Calibration noise	0.5	0.7
Total rms error	4.5%	6.5%

The data obtained have been plotted on a graph containing all absolute flux measurements that are now available. The results for Cassiopeia A were corrected to 1964.0, under the assumption of a secular decrease of 1.1 per cent per year in the flux, and the data are shown in Fig. IV-10. Similar results are shown in Fig. IV-11 for Taurus.

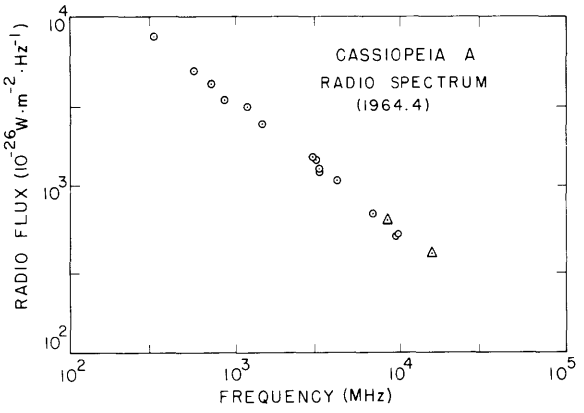

Fig. IV-10.

Radio spectrum of Cassiopeia A. Open circles denote other published values of greater than 10 per cent precision. The present measurements are indicated by open triangles.

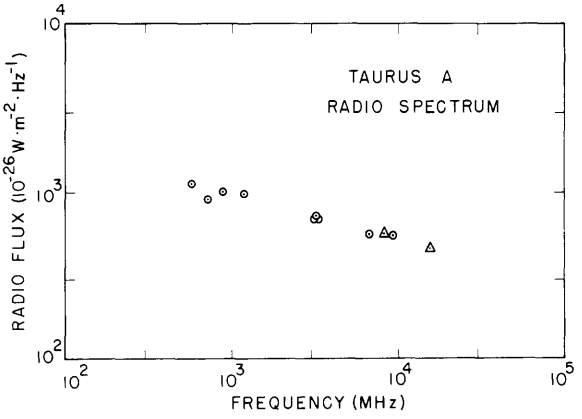

Fig. IV-11.

Radio spectrum of Taurus A. Data selected as in Fig. IV-10.

It is clear that the change in spectral index above 7 GHz for Cassiopeia A, as reported by Baars and his co-workers,[6] has not been found. The radio spectrum is well

approximated by a low of the form $X = k\nu^{-\alpha}$ (where ν = frequency, and k is some constant) for a constant value of $\alpha = 0.75 \pm .05$ over the entire range of data shown.

The data for Taurus also suggest a constant spectral index, α. The lower frequency value of 0.25 is in reasonable accord with the present results, although the data as a whole exhibit greater scatter from a smooth curve than for Cassiopeia.

The research described in this report has been made possible through the kind cooperation of the staff of the Haystack Research Facility, Lincoln Laboratory, M.I.T. We wish to acknowledge especially the assistance of John A. Ball, who made some of the 15.5-GHz observations and offered many helpful criticisms. Also, the data-reduction problem was greatly facilitated by the CDC 3200 computer, made available by J. Morriello, and by a paper-tape reading program provided by Patricia P. Crowther for the Univac 490 computer.

R. J. Allen, A. H. Barrett

References

1. R. J. Allen and A. H. Barrett, Quarterly Progress Report No. 81, Research Laboratory of Electronics, M.I.T., April 15, 1966, p. 13.
2. A. Sotiropoulos and J. Ruze, "Haystack Calibration Antenna," Technical Report No. 367, Lincoln Laboratory, M.I.T., Lexington, Mass., December 15, 1964.
3. H. G. Weiss, "The Haystack Experimental Facility," Technical Report No. 365, Lincoln Laboratory, M.I.T., Lexington, Mass., September 15, 1964.
4. These terminations are a manufactured item, consisting of a well-matched load in a styrofoam potentiometer. They have greatly facilitated the frequent calibrations of the radiometers.
5. J. W. Boland, J. P. Hollinger, C. H. Mayer, and T. P. McCullough, Astrophys. J. 144, 437 (1966).
6. J. W. M. Baars, P. G. Mezger, and H. Wendker, Astrophys. J. 142, 122 (1965).

B. RADIO DETECTION OF INTERSTELLAR $O^{18}H^1$

Previous radio observations of interstellar OH have been due to the most abundant istopic species $O^{16}H^1$. These observations have allowed the computation[1] of the detection possibilities and accurate line frequencies of the isotopic species $O^{18}H^1$. In particular, the F = 2→2, $^2\pi_{3/2}$, J = 3/2, Λ-doublet transition was calculated to occur at 1630.3 ± 0.2 Mc/sec. We have observed this line in the absorption spectrum of the galactic center (Sagittarius A) using the 140-ft radio telescope of the National Radio Astronomy Observatory. The observations were made during April 30-May 4, 1966, and consisted in a total of 18 hours of integration. The observations reveal absorptions of approximately 0.4°K and 0.1°K at radial velocities of +40 km/sec and - 135 km/sec, respectively, if the rest frequency is taken to be 1639.460 Mc/sec. The velocities of

absorption are in excellent agreement[2] with those of $O^{16}H^1$, and the rest frequency agrees very well with the predicted value. The results of the observations are shown in Fig. VI-12. A spectral width of 2.0 Mc/sec was the maximum that could be examined within our assigned time on the antenna. This also precluded making observations of the line expected at 1637.3 ± 0.2 Mc/sec which might be as much as a factor of two less intense and, therefore, require four times as much observing time for the same

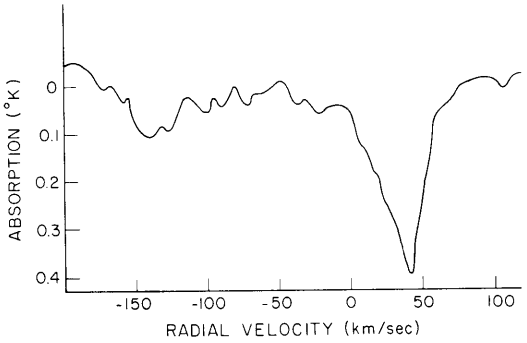

Fig. IV-12. $O^{18}H^1$ absorption profile in the direction of the galactic center (Sagittarius A).

$\Delta\nu$ (resolution), 50 kHz
τ = 18 hr
Theoretical rms, 0.03°K
Rest frequency, 1639.460 MHz.

signal-to-noise ratio.

The theoretical rms noise for 18 hours of integration is 0.03°K, and it is apparent that this valve is almost realized. Severe problems arise in spectral-line radiometers when very long integration times are involved. A dual-switching technique to eliminate instrumental effects was used. First, a load-switching technique was used on each hour of observation and the correlator computed the difference in autocorrelation functions looking at the antenna and then at the load. Then for each hour observation the local oscillator was shifted to displace any signal from Sagittarius A by 250 kc/sec, from the previous position in a three-position cycle. The data were then averaged by shifting the spectra appropriately so that the signals line up in frequency. The data were also averaged by using shifts opposite to those required to line up the signal data. The difference of the two averages was then taken and compensation made for the smeared signal data in the reference spectrum. This last technique eliminated any instrumental spectra from the correlator which amounted to several degrees. The instrumental effect in the correlator was due to the fact that errors in the sampler were not entirely random and independent of the load-switching cycle. This combination of load and frequency switching may always be desirable, however, for long integration times, even with improved samples performance.

It is difficult to estimate the O^{18}/O^{16} isotopic abundance ratio from the results of the observations because of some uncertainty in the interpretation of the $O^{16}H^1$ absorption. Robinson and co-workers[3] give an $O^{16}H^1$ optical depth of 0.9 for the +40 km/sec absorption feature in Sagittarius A, and similar arguments can be used to infer an

optical depth of 0.35 for the -135 km/sec feature if the more recent observations of Bolton and co-workers[2] are used. Our observations can be interpreted in terms of $O^{18}H^{1}$ optical depths of 2×10^{-3} and 5×10^{-4} for the +40 km/sec and -135 km/sec features, respectively. If we make the plausible assumption that the $O^{18}H^{1}$ and $O^{16}H^{1}$ dipole matrix elements are the same, and the more uncertain assumption that the $O^{18}H^{1}$ and $O^{16}H^{1}$ optical depths are in the direct ratio of the O^{18}/O^{16} abundances, then we derive O^{18}/O^{16} isotopic abundance ratios of 1/450 and 1/700 for the two absorption features. These are in good agreement with the terrestrial abundance ratio of 1/490. Departures of the interstellar ratios from the terrestrial value could easily be explained by the uncertainty in the observed data, interpretation of the $O^{16}H^{1}$ observations or different excitation and/or formation mechanisms for the two isotopic species of OH. To the best of our knowledge, the observations yield the first measure of any isotopic abundance ratios for the interstellar medium.

We wish to acknowledge the cooperation of personnel of the National Radio Astronomy Observatory and the use of the 140-ft radio telescope for our observations.

A. H. Barrett, A. E. E. Rogers

References

1. A. H. Barrett and A. E. E. Rogers, Nature 204, 62 (1964).
2. J. G. Bolton, F. F. Gardner, R. X. McGee, and B. J. Robinson, Nature 204, 30 (1964).
3. B. J. Robinson, F. F. Gardner, K. J. van Damme, and J. G. Bolton, Nature 202, 989 (1964).

C. K-BAND MEASUREMENTS

Measurements of Venus, Jupiter, the Sun, Moon, Taurus A, and 3C273 were made during the period from January to March, 1966, at wavelengths of 1.18, 1.28, 1.35, 1.43, and 1.58 cm. The five-channel Dicke radiometer and 28-ft antenna were essentially those described in a previous report.[1] The major additions to the system were IF gain modulators to permit separate balancing of each channel, and a new antenna feed to permit operation at lower frequencies.

The preliminary results indicate that the average spectra of Venus and Jupiter exhibited no resonant features at the 1.35-cm wavelength water-vapor resonance.

D. H. Staelin, N. E. Gaut, R. W. Neal,
G. D. Papadopoulos, E. C. Reifenstein

References

1. D. H. Staelin and A. H. Barrett, Quarterly Progress Report No. 78, Research Laboratory of Electronics, M.I.T., July 15, 1965, p. 21.

D. ATMOSPHERIC ABSORPTION AT 72 Gc/sec

An experiment to measure the atmospheric opacity at 72 Gc/sec was performed to investigate absorption on the wings of the millimeter resonance lines of molecular oxygen. Solar-extinction measurements were made with the 4-mm radiometric system on the roof of Building 26 at M.I.T., in Cambridge. Radiosonde measurements of the temperature, pressure, and water-vapor density profiles were obtained from the Aerospace Instrumentation Laboratory at the Air Force Cambridge Research Laboratories for the days of the observations.

On a clear day, the total atmospheric opacity, τ, at 72 Gc/sec will be the sum of the opacities arising from molecular oxygen absorption and water-vapor absorption.

$$\tau = \tau_{O_2} + \tau_{H_2O}. \tag{1}$$

Generally, τ_{H_2O} is of the order of 1/3-1/2 of τ_{O_2} at this frequency for typical winter atmospheres. For each of the days of observation, theoretical values of the opacity, based on the radiosonde data, were computed for comparison with the measured opacities. The opacity resulting from water-vapor absorption was computed by using the absorption coefficient of Barrett and Chung[1] as modified by Staelin.[2] Two separate oxygen opacities were computed for each observing day. In one, the resonance line shape of Van Vleck and Weisskopf,[3]

$$F_{vv-w}(\nu, \nu_o, \Delta\nu) = \frac{\nu}{\pi\nu_o}\left[\frac{\Delta\nu}{(\nu-\nu_o)^2 + \Delta\nu^2} + \frac{\Delta\nu}{(\nu+\nu_o)^2 + \Delta\nu^2}\right], \tag{2}$$

was used for each of the millimeter resonance lines of oxygen; in the other, the line shape of Zhevakin and Naumov,[4]

$$F_{Z-N}(\nu, \nu_o, \Delta\nu) = \frac{4\nu\nu_o}{\pi} \frac{\Delta\nu}{\left(\nu^2-\nu_o^2\right)^2 + 4\nu^2\Delta\nu^2}, \tag{3}$$

was used. The expression for the linewidth parameter, $\Delta\nu$, appearing in both the line-shape expressions was taken as that of Meeks and Lilley.[5]

Table IV-9 shows the measurements compared with each of the theoretical computations.

Table IV-9. Atmospheric opacities.

$$\tau_{vv-w} = \tau_{O_2}{}_{vv-w} + \tau_{H_2O}$$

$$\tau_{z-n} = \tau_{O_2}{}_{z-n} + \tau_{H_2O}$$

	τ measured (db)	τ_{vv-w} (db)	τ_{z-n} (db)
18 March 1966	1.71 ± 0.15	2.09	1.83
21 March 1966	1.29 ± 0.21	1.94	1.66
29 March 1966	1.37 ± 0.17	1.67	1.35
4 April 1966	1.65 ± 0.23	1.84	1.59
15 April 1966	1.62 ± 0.19	1.94	1.68

The measurements appear to be in fairly good agreement with the computations based on the Zhevakin-Naumov line shape. It is possible, however, to explain the measured results within the context of the Van Vleck-Weisskopf line shape if the linewidth parameter, $\Delta\nu$, is taken as 0.85 of the value used in the computations. At the pressures of interest this is not an unreasonable value for $\Delta\nu$.

Atmospheric opacity measurements both above and below the 60 Gc/sec complex of oxygen lines are suggested to resolve this conflict. The line-shape difference is an asymmetric one, with the VV-W line shape giving more absorption above the resonance and less below it than the Z-N line shape; whereas a smaller $\Delta\nu$ gives less absorption both above and below the resonance.

Also, recent laboratory measurements of the millimeter and submillimeter

water-vapor lines should be incorporated into a more accurate expression for absorption at frequencies near 72 Gc/sec.

P. R. Schwartz, W. B. Lenoir

References

1. A. H. Barrett and V. K. Chung, J. Geophys. Res. 67, 4259-4266 (1962).
2. D. H. Staelin, Sc. D. Thesis, Department of Electrical Engineering, M. I. T. February 1965.
3. J. H. Van Vleck and V. F. Weisskopf, Rev. Mod. Phys. 17, 227-236 (1945).
4. S. A. Zhevakin and A. P. Naumov, Radio teknika i Elektronika 9 (8), 1327 (1964).
5. M. L. Meeks and A. E. Lilley, J. Geophys. Res. 68, 1683-1695 (1963).

E. OBSERVATIONS OF MICROWAVE EMISSION FROM ATMOSPHERIC OXYGEN

The data taken during the balloon flights in July, 1965, have been reduced.[1] The results of the ascent portion of Flight 154-P are shown in Fig. IV-13. The solid lines are theoretical computations based on the Van Vleck-Weisskopf pressure-broadened

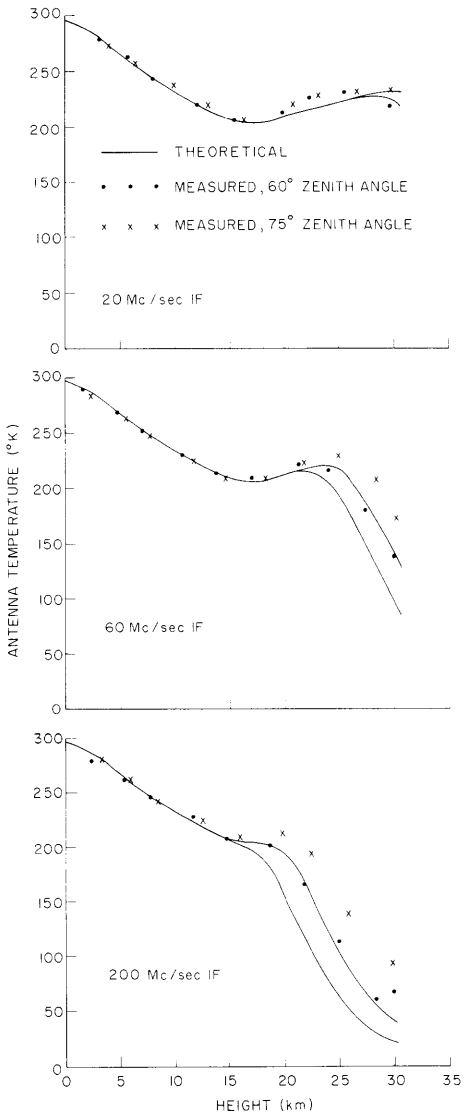

Fig. IV-13. Results of ascent part of Flight 154-P.

resonance line shape. The true atmospheric temperature profile (as measured on ascent) was used in the theoretical computations.

The data of Fig. IV-13 are generally consistent with those taken during previous balloon flights.[2] The theoretical antenna temperatures agree with the measured values for low heights, at which both are equal to the atmospheric temperature because the optical

depth is large for all channels. The antenna temperatures of the 200-Mc/sec channels are the first to depart from the atmospheric temperature at ~18-20 km; the antenna temperatures of the 60-Mc/sec and 20-Mc/sec channels do likewise at 22-24 km and 28-30 km, respectively.

Differences between the measured and theoretical values are evident. On the 200-Mc/sec and 60-Mc/sec channels the measured antenna temperatures are higher than predicted above the height at which departure from the atmospheric temperature occurs;

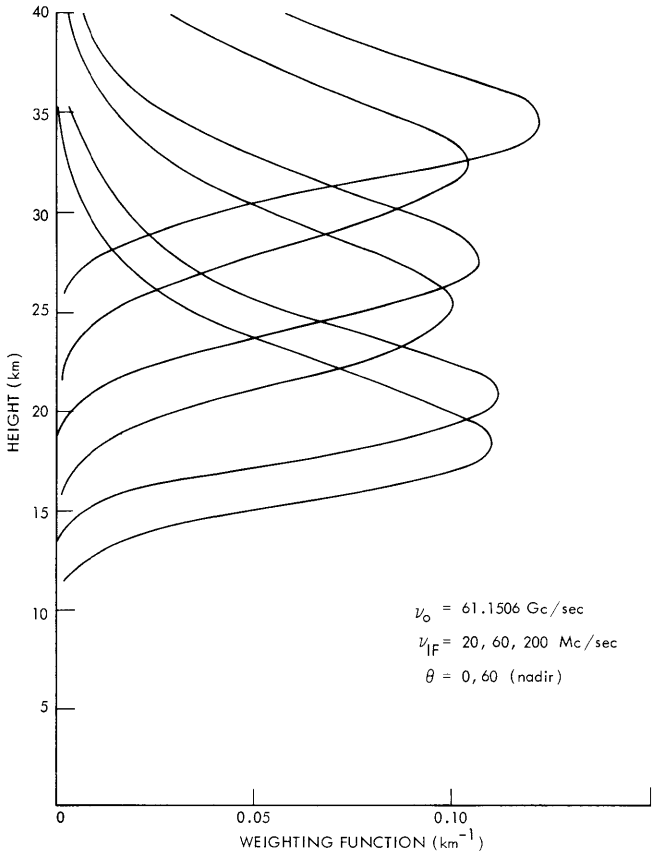

Fig. IV-14. Temperature weighting functions for Flights 152-P and 153-P.

Table IV-10. Summary of Winter balloon flight experiments.

Flight	Date	Duration	Float Altitude	Comments
198-LP	27 Jan.	8 hr	38 km	Successful
199-LP	2 Feb.	1 1/2 hr	none	Beacon Failure
200-LP	3 Feb.	8 hr	39 km	Successful

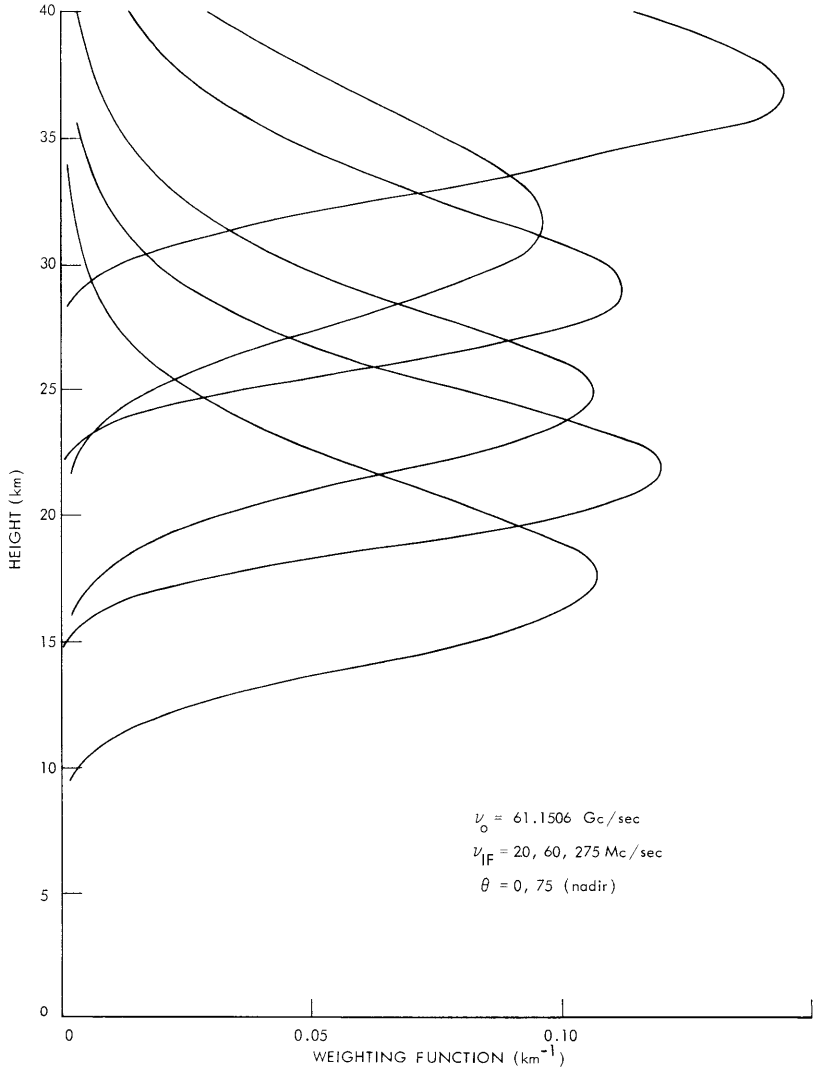

Fig. IV-15. Weighting functions for Flights 198-LP, 199-LP, and 200-LP.

whereas the 20-Mc/sec channels behave approximately as predicted by theory. These results would appear to indicate a higher absorption than predicted at ±200 Mc/sec and ±60 Mc/sec from the resonance frequency, and an absorption equal to the predicted value at ±20 Mc/sec from the resonance.

The discrepancy may lie in the theoretical assumption that the absorption coefficient resulting from many overlapping resonance lines is the sum of the individual absorption coefficients. There has been some evidence that this is not the case in the wings of overlapping lines, but that the true absorption coefficient is larger than the sum of the individual ones.

Analysis of the data from Flight 154-P continues; in particular, an inversion

Table IV-11. Summary of Flights 198-LP, 199-LP, and 200-LP.

ν_o = 61.1506 Gc/sec (local-oscillator frequency)

$\Delta T_{rms} \sim$ 1-2°K

ν_{if} = center frequency of IF passband

BW_{if} = bandwidth of IF passband

h_o = height of weighting-function maximum

Δh = width of weighting function

T_B = brightness temperature predicted from model atmosphere

θ = angle of antenna direction (from nadir)

θ (deg)	ν_{if} (Mc/sec)	BW_{if} (Mc/sec)	h_o (km)	Δh (km)	T_B (°K)
75	20	10	37	7	258
0	20	10	32	10	246
75	60	10	29	8	244
0	60	10	25	9	230
75	275	24	22	7	222
0	275	24	17.5	8	218

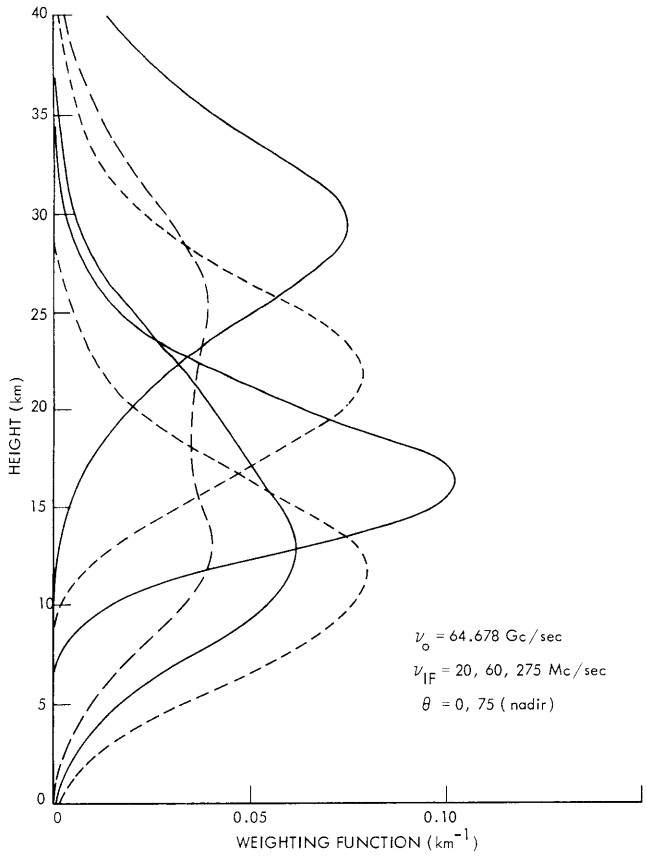

Fig. IV-16.
Predicted weighting functions for flights in Summer, 1966.

method yielding the absorption coefficient at various heights for each of the channels is being developed. This information will make interpretation in terms of correct line shapes much easier.

The results of Flights 152-P and 153-P are being analyzed with emphasis on inverting the microwave antenna temperature measurements to obtain the atmospheric temperature profile in the 16-38 km height range. The temperature weighting functions for these flights are shown in Fig. IV-14.

Another series of balloon flights was undertaken in January-February, 1966, from Phoenix, Arizona. The purpose of these flights was similar to that for Flights 152-P and 153-P, namely to make microwave measurements that could be interpreted to yield the atmospheric temperature profile for a given height range. The flight characteristics and comments are summarized in Table IV-10. The weighting functions for these flights are shown in Fig. IV-15. The radiometer was modified slightly to give a better spread of weighting functions and to probe as deeply as possible for frequencies centered on the 9+ resonance line. The radiometer parameters and the height levels sounded by these experiments are summarized in Table IV-11. Analysis of these data is under way.

Table IV-12. Summary of flights in Summer, 1966.

ν_o = 64.678 Gc/sec

ΔT_{ems} 1-2°K

θ (deg)	ν_{if} (Mc/sec)	BW_{if} (Mc/sec)	h_o (km)	Δh (km)	T_B (°K)
75	20	10	29	12	231
75	60	10	22	12	218
75	275	24	16	9	214
0	20	10	14-25	23	225
0	60	10	13	15	224
0	275	24	12	11	227

Future flights are planned for the summer of 1966. Major changes in the radiometer are being made; the local-oscillator frequency is being changed to 64.678 Gc/sec, the 21+ resonance which is much weaker than the 9+ resonance, and the three IF will be operated simultaneously rather than singly. The new frequency will permit weighting functions that penetrate the tropopause to give inversion methods a real test.

The predicted weighting functions for these flights are shown in Fig. IV-16. The radiometer parameters and the height levels sounded by these experiments are summarized in Table IV-12.

W. B. Lenoir

References

1. W. B. Lenoir, Quarterly Progress Report No. 79, Research Laboratory of Electronics, M.I.T., October 15, 1965, pp. 17-19.

2. A. H. Barrett, J. W. Kuiper, and W. B. Lenoir (submitted to J. Geophys. Res.).